

# Surface Physical Structure and Durability of Superhydrophobic Wood Surface with Epoxy Resin

Fan Kang,<sup>a,b</sup> Zede Yi,<sup>a</sup> Bo Zhao,<sup>a</sup> and Zhiyong Qin<sup>a,\*</sup>

In this study, a superhydrophobic wood surface was prepared with amino-functionalized nano-silica (SiO<sub>2</sub>) particles, epoxy resin (EP) of different curing times, and octadecyltrichlorosilane (OTS). The micro-nano structures of the wood samples were represented by scanning electron microscopy (SEM), while the hydrophobicity and durability of the hydrophobic effect was shown by the contact angle (CA) tests. The results indicated that the optimal curing time of EP was 4 h, such that the wood surface exhibited promising superhydrophobicity with a static CA of 155.4° and a sliding angle (SA) of 3.9°. The different curing time of EP had a remarkable influence on the roughness and the pore structure type of superhydrophobic wood surface. In terms of the Cassie-Baxter theory, the increase of CA on the wood surface was ascribed to the presence of secondary air pores and rough structure in the solid-liquid interface. The obtained wood surface not only possessed excellent adhesion stability and anti-aging properties, but also a resistance to acidic solutions, organic solvents, and mechanical abrasion.

*Keywords:* Superhydrophobic wood; Epoxy resin; Curing time; Structural model; Micro-nano rough surface

*Contact information:* a: School of Resources, Environment and Materials, Guangxi University, Nanning 530000, China; b: School of Materials Science and Engineering, South China University of Technology, Guangzhou 510640, China; \*Corresponding author: qinzhuyong@gxu.edu.cn

## INTRODUCTION

As an environmentally friendly material, wood is widely used in the fields of wooden structure architectural design, furniture manufacturing, and interior/exterior decoration. However, cellulose and hemicellulose as the main components in wood have abundant hydrophilic groups, which easily adsorb external water molecules through hydrogen bonding (Aggarwal *et al.* 2015). In addition, the porous structure of wood provides rich channels for moisture migration (Zhao *et al.* 2020). Because of the undesired properties, wood is susceptible to mildew, decay, and degradation, which limits the use of wood and reduces the service life of wood (Armingier *et al.* 2019). To reduce the hygroscopicity caused by porous structures and hydrophilic groups of wood, many methods have been employed for wood external and internal protection (Barthlott and Neinhuis 1997). Meanwhile, the application of superhydrophobic modification for wood is proposed to overcome the above challenges. The wood surface was endowed with unique wettability and improved the functional properties, such as water resistance, dimensional stability, *etc.*, which further broadens wood multifunctional usage (Yi *et al.* 2020).

The so-called superhydrophobic surface is defined as the surface where the contact angle (CA) of a water droplet is greater than 150° and the sliding angle (SA) is less than 10° (Xue *et al.* 2009; Wang *et al.* 2012; Sahoo and Kandasubramanian 2014; Parvate *et al.* 2020). The best known examples of superhydrophobicity in nature are species such as lotus

leaves, rose petals, water strider legs, and butterfly wings (Neinhuis and Barthlott 1997; Feng *et al.* 2008; Wagner *et al.* 2010; Liu *et al.* 2015b). Micron-scale or nano-level rough structures and hydrophobic wax are found on their surface. Thus, the superhydrophobic phenomenon is attributed to the interaction between micro-nano structures and low-surface-energy materials. To this purpose, methods, such as sol-gel, layer-by-layer self-assembly, hydrothermal treatment, *etc.*, are suitable for biomimetic construction of wood superhydrophobic surface and have been reported (Wang *et al.* 2011; Wu *et al.* 2016; Lukawski *et al.* 2018; Xing *et al.* 2018; Wang *et al.* 2019).

According to previous papers, the application of biomimetic construction on the surface of superhydrophobic wood has been investigated. Jia *et al.* (2016) enriched silica nanoparticles modified by vinyltriethoxysilane (VTES) on prefabricated wood to obtain superhydrophobic surface with admirable wear resistance. Similarly, Wang *et al.* (2017) developed the roughness and free energy was modified by copper plating and octadecylamine (ODA) on the microsphere substrate where it has attached poly-dopamine, and the CA of water on the wood surface was 157°. The composite coating of alumina-polydimethylsiloxane (PDMS) was produced by solvent and non-solvent process for the wood protection, which made water absorption in wood decrease at most 28% (Shah *et al.* 2017). Furthermore, Wang *et al.* (2020b) have obtained such wood surface with the formation of fluoroalkylsilane/silica composite coating, which exhibits excellent superhydrophobicity with self-healing and good resistance to abrasion.

However, a physical combination between a substrate surface and inorganic nanoparticles has been mainly adapted to prepare superhydrophobic surfaces in traditional strategies, but the stability of micro-nano rough structure has been neglected in practical application (Han *et al.* 2019; Zhan *et al.* 2019). Moreover, the superhydrophobic wood surfaces are easily damaged by environmental factors such as light intensity, rain, and microbial decomposition (Tenjimbayashi and Shiratori 2014). The coatings are rubbed and impacted by mechanical operations during processing and use, resulting in the hydrophilic layer on the surface being exposed to the air. The superhydrophobic surface also has been lacking durability (Lu *et al.* 2019; Yang *et al.* 2019, 2020), so finding a polymer with promising adhesion performance for introducing chemical bonds to improve the interfacial bonding of micro-nano structure and substrate has gained interest among researchers.

As a strong adhesion polymer, epoxy resin (EP) was selected on account of chemical bonds being generated by the reaction among the epoxide group, modified particles, and free bonds of wood surface (Liu *et al.* 2019; Tuong *et al.* 2019). The cured EP is characterized by mechanical stability, water repellency, and corrosion resistance (Psarski *et al.* 2019; Xu *et al.* 2019; Zhou *et al.* 2019), which may improve the stability of a superhydrophobic surface. Therefore, epoxy-based superhydrophobic wood products are suitable for kitchen countertops, chopping boards and balcony guardrails, which can effectively prolong the service life of these wood products.

Inspired by the chemical connection formed through the ring opening reaction with the amino group and the epoxide group, Liu *et al.* (2015a) reported that the silica particles were modified by 3-triethoxysilylpropylamine (APS) and fabricated mechanical stability of superhydrophobic coatings anchored by the cured EP. The researchers used polyvinyl alcohol (PVA) as a coating polymer, and then the PVA/SiO<sub>2</sub> composite coatings with the mechanical robustness were prepared by the above method (Liu *et al.* 2013). In addition, Wang *et al.* (2020c) fabricated such a surface by grafting poly 2-perfluorooctyl ethyl methacrylate (PFOEMA) onto wood by atom transfer radical polymerization (ATRP). According to the existing literature on superhydrophobic polymer coating, research has

focused on different resin types and addition amounts (Liu *et al.* 2011; Su *et al.* 2017; Tu *et al.* 2018), but differences in the curing time of the polymer are rarely reported. The focus is only considered to the effect of resin on the coating, which ignores resin with a different curing time, which may cause the change of superhydrophobic rough structure. In this study, the highlight is the effect of EP on the superhydrophobic property based on a different curing time.

The present study aimed to prepare epoxy-based coating with the best curing time and finally obtain a stable and durable superhydrophobic wood surface. The wood samples were fabricated in a three-step process: (1) The wood was impregnated with EP in vacuum for different curing times, (2) the epoxide wood surface was modified by amino-functionalized nano-silica (SiO<sub>2</sub>) particles to increase roughness, and (3) a low-surface-energy layer on the wood surface was constructed by fluoride-free octadecyltrichlorosilane (OTS) reagent (Kumar *et al.* 2018). Moreover, the stability, aging resistance, acid-base resistance, and mechanical stability of the surface coating were evaluated through the determination of simulated rain, durability, chemical stability, ultrasonic vibration, and direct abrasion of the wood surface. A scanning electron microscope (SEM) was used to characterize the microstructure of superhydrophobic wood surface; the hydrophobic and durability properties of the treated sample were characterized by measuring static droplet's CA.

## EXPERIMENTAL

### Materials

*Pinus sylvestris* wood samples were obtained from Shanghai Jimuwu Co., Ltd. (Shanghai, China) and machined into 20 mm (longitudinal) × 10 mm (tangential) × 5 mm (radial) pieces. Bisphenol A epoxy resin precursor part-A and polyamide curing agent part-B were provided by Nantong Xingxing Synthetic Materials Co., Ltd. (Nantong, Jiangsu, China). The OTS and 3-aminopropyltriethoxysilane (KH550) were purchased from Shanghai Aladdin Chemistry Co., Ltd. (Shanghai, China). Hydrophilic SiO<sub>2</sub> particles with a diameter of 15 ± 5 nm were obtained from Shanghai Keyan Industrial Co., Ltd. (Shanghai, China). Ethanol (99.0%), N,N-dimethylformamide, acetone, n-hexane (98.0%), hydrochloric acid (HCl), and sodium hydroxide (NaOH) were produced from Funing Fine Chemical Co., Ltd. (Tianjin, China). Ink solution of black dyes was obtained from Nanchang Yongxiang Culture Co., Ltd (Jiangxi, China). Methyl orange was purchased from Shanghai McLean Biochemical Technology Co., Ltd (Shanghai, China) and prepared a dilute solution of 50 mg/L. Deionized water was self-made in the laboratory. All of the chemicals were used as received without further purification.

To remove residual wood flour, surface stains, and grease, the wood samples were washed with ethanol and deionized water by an ultrasonic cleaner for 20 min. The samples were used after oven-drying at 80 °C for 24 h.

### Modification of SiO<sub>2</sub> Particles

The amino groups were introduced by grafting KH550 onto the original SiO<sub>2</sub> particles, which was beneficial to form the chemical bonds between the particles and EP. The KH550 hydrolysate was prepared by mixing 4 g KH550 and 196 g ethanol solution (95.0%, w/w) with magnetic stirring at room temperature for 30 min. Subsequently, 2 g SiO<sub>2</sub> particles were dispersed into the hydrolysate by further stirring at 60 °C for 6 h.

Ultimately, the modified  $\text{SiO}_2$  particles were separated by centrifugation (TG16-WS, 6\*50ml) with a speed of 8000 r/min and washed with ethanol and deionized water three times for 10 min each time to remove the unreacted KH550. The amino-functionalized  $\text{SiO}_2$  ( $\text{SiO}_2\text{-NH}_2$ ) particles were used after drying at  $60^\circ\text{C}$  for 12 h. The entire preparing process of  $\text{SiO}_2\text{-NH}_2$  particles can be seen in Fig. 1.

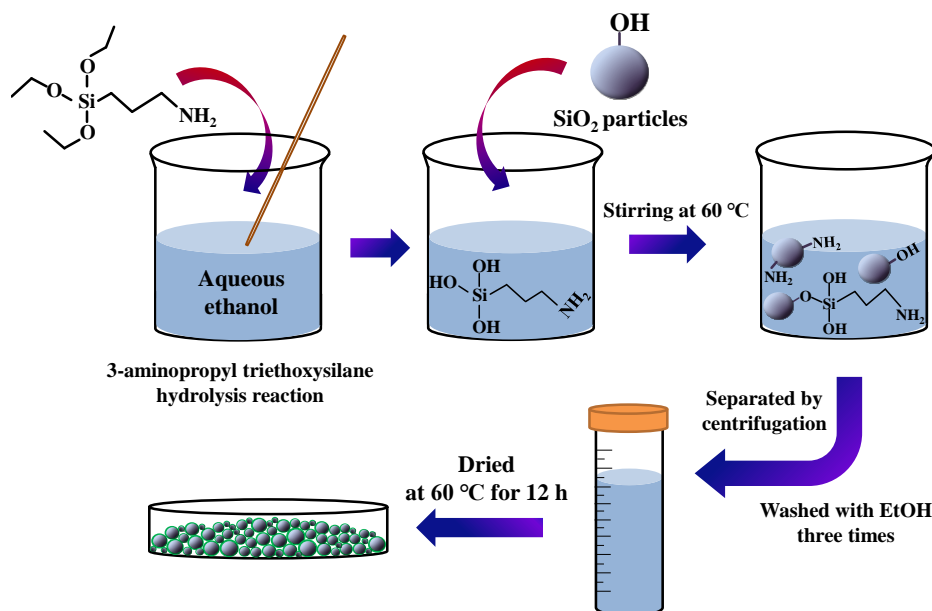


Fig. 1. Preparation of  $\text{SiO}_2\text{-NH}_2$  particles

### Fabrication of EP/ $\text{SiO}_2\text{-NH}_2$ Coating and Treatment of Low Surface Energy on Wood Surface

To improve the stability of the nanoparticles on the wood surface, EP was used to connect the wood surface with the rough structure. The  $\text{SiO}_2\text{-NH}_2$  particles were used to prepare the micro-nano rough structures on the wood surface. The EP solution was obtained by mixing precursor part-A (40.5 g), polyamide curing agent part-B (13.5 g), and ethanol (126 g) and being stirred at the room temperature. The wood samples were immersed into the solution in a sealed container with atmospheric pressure of 0.8 MPa. After being maintained for 30 min, the samples were placed at room temperature for further use. The samples were labelled as Wood@EP.

Next, 1% (w/w)  $\text{SiO}_2\text{-NH}_2$  suspension was treated by ultrasonic dispersion (TL-650Y; Jiangsu Tianling Instrument Co., Ltd., Jiangsu, China) in an ice bath for 10 min with a power of 400 W. Each group of Wood@EP samples was cured with the time of 0, 0.5, 1, 2, 4, 8, and 24 h at room temperature, and then EP/ $\text{SiO}_2\text{-NH}_2$  coating was obtained on the samples' surfaces that immersed the suspension for 10 min to construct the roughness structure. The Wood@EP/ $\text{SiO}_2\text{-NH}_2$  samples were dried at  $60^\circ\text{C}$  for 24 h to ensure the complete curing of the EP. To evaluate the effect of EP on the composite coating, a contrast experiment was set up and the wood samples were prepared without EP. The labelled Wood@ $\text{SiO}_2\text{-NH}_2$  samples were obtained by treatment of the suspension for 10 min and drying at  $60^\circ\text{C}$  for 24 h.

The 2 wt% OTS solutions were prepared with n-hexane. The Wood@EP/ $\text{SiO}_2\text{-NH}_2$  and Wood@ $\text{SiO}_2\text{-NH}_2$  samples were immersed into OTS solution and stirred by magnetic force for 2 h, which grafted the surface with long chain silane to low energy. Then, the

superhydrophobic samples were obtained after drying for 24 h at room temperature, as depicted in Fig. 2. For the convenience of distinction, the wood samples prepared by the above methods were respectively recorded as Wood@EP/SiO<sub>2</sub>-NH<sub>2</sub>&OTS and Wood@SiO<sub>2</sub>-NH<sub>2</sub>&OTS.

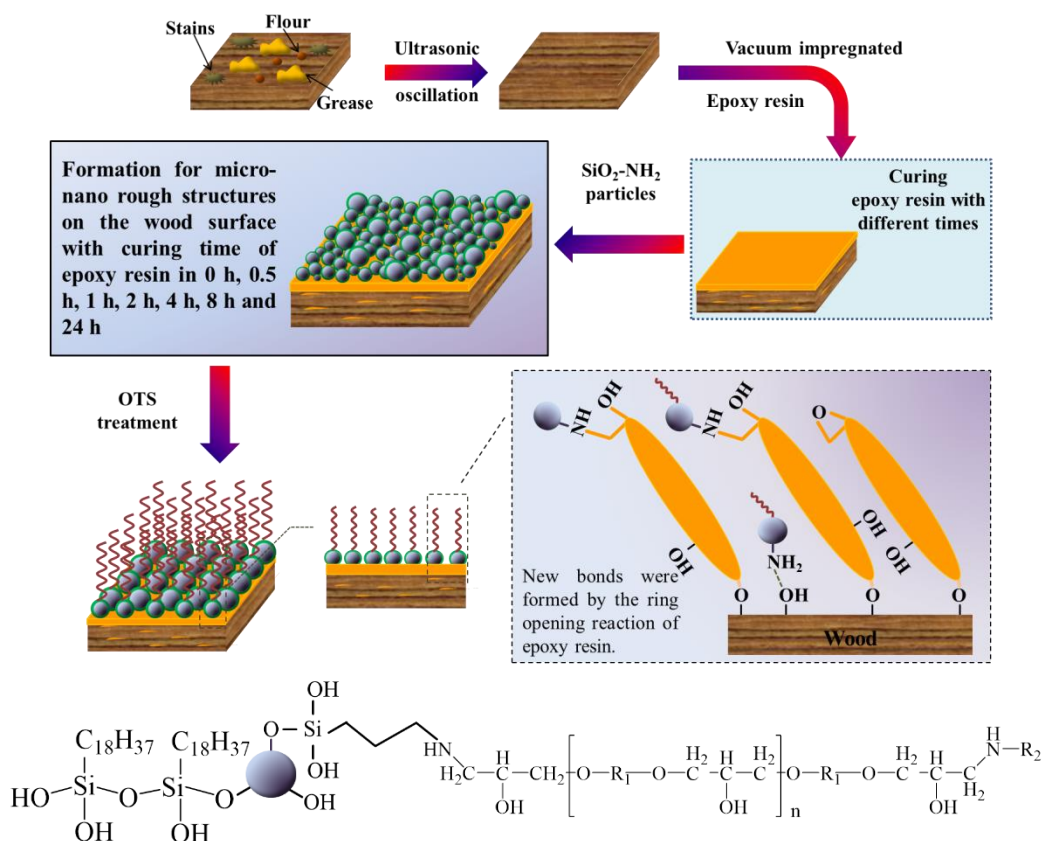
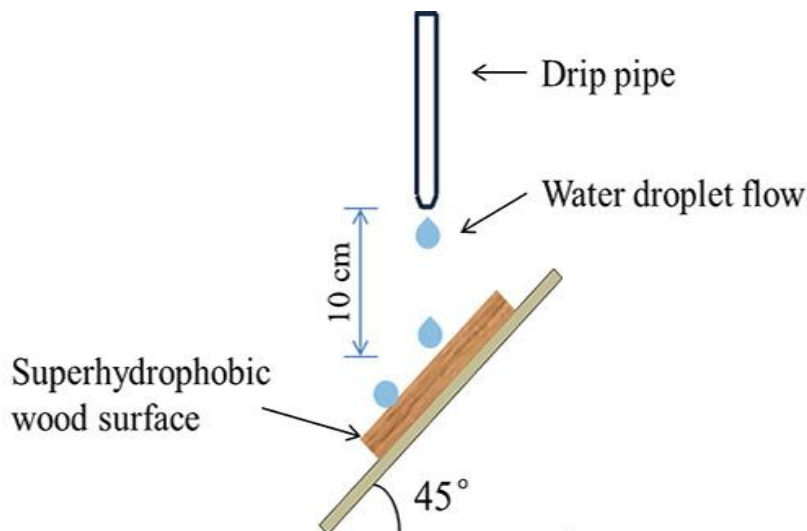


Fig. 2. Processes and reaction mechanism of fabricating superhydrophobic wood

### Characterization

The static CA and CA hysteresis were performed with a CA meter (KRÜSS DSA100E, Hamburg, Germany). The wettability of wood samples was analyzed by measuring the water CAs with 3 μL droplets at room temperature. The dynamic process of droplets contacting the wood surface was recorded, and the first 6 s were adopted for data analysis. The SAs were determined by the minimum inclination angle at which a 3 μL droplet rolled off the sample surface. Five positions of each sample were measured, and the averages were taken. The surface morphologies of wood samples were characterized by SEM (QUANTA200, FEI, Hillsboro, OR, USA) operating at 5 kV.

To simulate the mechanical force and wettability by the impact of rainfall, the test on the surface of the samples was set up at a constant water flow speed, as shown in Fig. 3. The Wood@EP/SiO<sub>2</sub>-NH<sub>2</sub>&OTS and Wood@SiO<sub>2</sub>-NH<sub>2</sub>&OTS samples were respectively fixed at 45° to the horizontal surface and the sample surface was 10 cm away from the drip pipe. The CA changes of the flow area were analysed after the test of 3 h, 6 h, 9 h, 12 h, 18 h, and 24 h.



**Fig. 3.** Sketch of simulated rain test

To study the aging resistance of composite coating, the wood samples were treated by ultraviolet light in different irradiation time. The Wood@EP/SiO<sub>2</sub>-NH<sub>2</sub>&OTS and Wood@SiO<sub>2</sub>-NH<sub>2</sub>&OTS samples were irradiated 10 cm below the ultraviolet light (WFH-204B, 300 W, 300 nm) at continuous irradiation time of 3, 6, 12, 18, and 24 h. In addition, considering the factor of temperature to anti-aging wood surface, other wood samples were oven-dried at 60 °C for 3, 6, 12, 18, and 24 h. All the CAs of the samples in each group were measured after the treatment.

The samples were treated with acid-base solution and organic solvents to evaluate the chemical stability of the wood surface. Deionized water, HCl (pH = 2, 4) solution, and NaOH (pH = 9, 12) solution were separately configured to be 50 mL. Meanwhile, 50 mL organic solvents, such as acetone, n-hexane, N,N-dimethylformamide, and ethanol, were prepared. The Wood@EP/SiO<sub>2</sub>-NH<sub>2</sub>&OTS and Wood@SiO<sub>2</sub>-NH<sub>2</sub>&OTS samples were immersed in the above solutions for 24 h and then were taken out and dried at 60 °C. The CAs of the surface after treatment of different acid-base solution and organic solvents were respectively measured, and the average values were taken as a reference.

To study the effect of ultrasonic vibration on adhesion SiO<sub>2</sub> particles in micro-nano construction, the Wood@EP/SiO<sub>2</sub>-NH<sub>2</sub>&OTS and Wood@SiO<sub>2</sub>-NH<sub>2</sub>&OTS samples were put into the water and vibrated in the ultrasonic vibration (KQ2200, Kunshan Ultrasonic Instrument Co., Ltd., China) with power of 100 W for 1, 2, 3, 4, 5, and 6 h. Then the wood samples were oven-dried at 60 °C for 30 min. The droplets CAs on the surface were measured and averaged after the ultrasonic treatment.

The abrasion resistance test for the determination of the mechanical stability is as follows. 600 mesh sandpaper served as the abrasive surfaces, with the surface of Wood@EP/SiO<sub>2</sub>-NH<sub>2</sub>&OTS and Wood@SiO<sub>2</sub>-NH<sub>2</sub>&OTS samples to be tested facing this abrasion material. While the 200 g weight was applied to the superhydrophobic wood surface, the surface was moved in one direction for 20 cm each time. The CA changes of the times of circulating movement were analysed after the test of 1, 3, 5, 10, 20, and 50 times, respectively.

## RESULTS AND DISCUSSION

### Wettability of the Wood Surface

Figure 4 shows a wetting state with methyl orange solution, water, and ink droplets on the treated wood surface, where the droplets present a ball-like appearance. The precise wettability was evaluated by the CAs and the SAs measurement of the wood surface for each curing time of EP, as shown in Fig. 5. Clearly, the Wood@EP/SiO<sub>2</sub>-NH<sub>2</sub>&OTS samples obtained superhydrophobic surface successfully *via* the experimental methods. The CAs emerged as an upward trend with respect to curing time of EP from 0 h to 4 h, and the optimal surface of superhydrophobic wood with the CA of 155.4° and the SA of 3.9° was obtained at 4 h. Compared with it, the curing time of EP was 8 h where the CA of the wood surface decreased 3.2°. Nevertheless, after the curing time reached 24 h, the CA had little effect. In this paper, the best curing times of EP for the wood preparation was judged to be 4 h, at which point the specimens showed outstanding superhydrophobic performance.



**Fig. 4.** Diagram of the static droplets (methyl orange, water, and ink) on the superhydrophobic wood surface

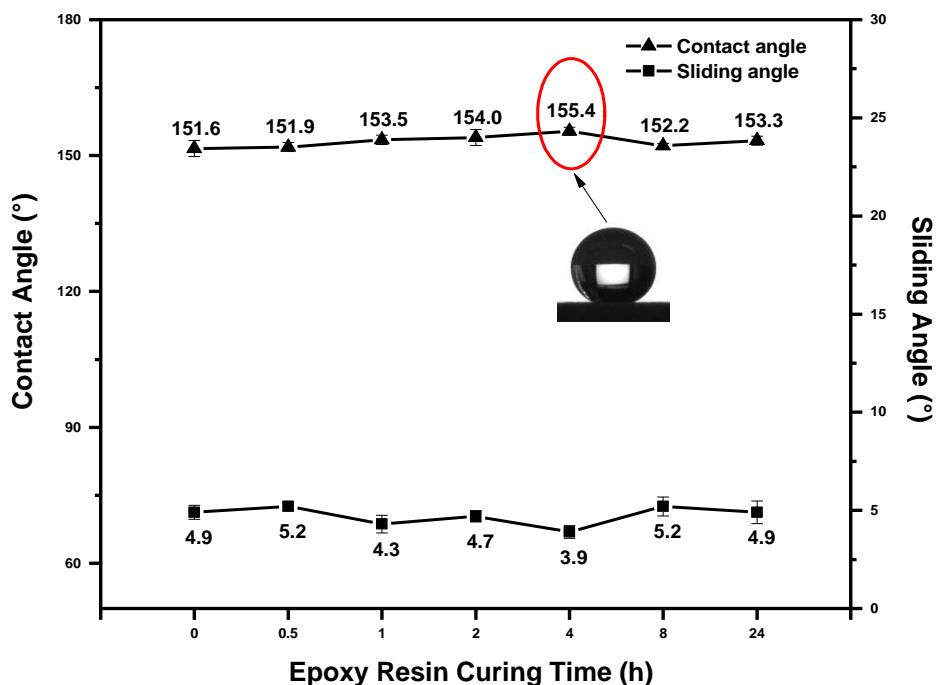


**Fig. 5.** Effect of EP curing time on CAs and SAs of wood surface

### Microstructure of the Superhydrophobic Surface

Figure 6 (a through f, a' through f') shows the structure change of wood surface in the different curing times of EP and the untreated wood. The cell wall and micro-grooves of the contrast wood were observed in Fig. 6a and a', which revealed *Pinus sylvestris* wood was a type of porous material with a smooth surface. As shown in Fig. 6b and b', the EP was not cured, the SiO<sub>2</sub> particles were covered with the resin, and the wood surface was adhered by EP/SiO<sub>2</sub>-NH<sub>2</sub>&OTS coating with the voids and few coarse particles. Figure 6c and c' show that a relatively dense coating was formed on the surface of the Wood@EP/SiO<sub>2</sub>-NH<sub>2</sub>&OTS samples with curing for 0.5 h, and the filamentous rough structures emerged. It could be seen from Fig. 6d,d' and e,e' that as the curing time of EP increased, a micro-nano rough structure with staggered height was formed by the SiO<sub>2</sub>-NH<sub>2</sub> particles on the surface. The area of filaments on the surface was gradually expanded, which was conducive to degrading the actual contact area between the water droplets and the surface coating.

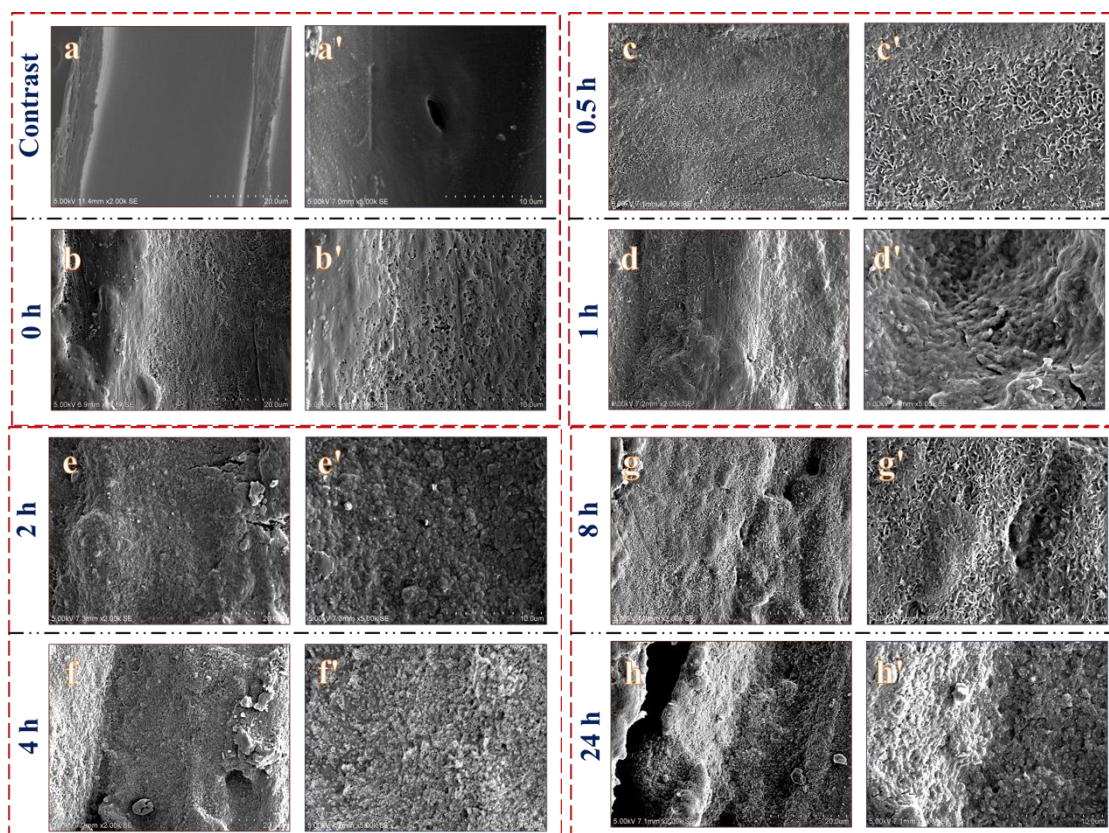


**Fig. 6.** SEM images of (a) and (a') are pristine *Pinus sylvestris* wood surface. The synthesized superhydrophobic Wood@EP/SiO<sub>2</sub>-NH<sub>2</sub>&OTS for different curing time are followings: (b)/(b') 0 h; (c)/(c') 0.5 h; (d)/(d') 1 h; (e)/(e') 2 h; (f)/(f') 4 h; (g)/(g') 8 h; and (h)/(h') 24 h. The wood surface topography was observed in magnifications of 2.00K for (a) (b) (c) (d) (e) (f) (g) (h) and 5.00K for (a') (b') (c') (d') (e') (f') (g') (h').

Figure 6f depicts the microstructure of superhydrophobic wood surface after curing EP for 4 h. The abundant nano-scale rough structures were formed on the wood surface, where a large number of subtle voids were observed as shown in Fig. 6f'. Compared with the superhydrophobic coating of EP/nanoparticles, to investigate the reasons for this phenomenon, a large number of pores were found on the surface after vacuum



impregnation (Liu *et al.* 2013, 2019). This might be caused by the full adhesion of the EP to the wood surface or interior in the vacuum state, while the anhydrous ethanol was released from the adhesive. The aggregation of EP and the formation of micro-nano structure were promoted by the modified particles; thus, air could be trapped in these cavities. This situation further reduced the wettability of the wood surface and enhanced its hydrophobic property to achieve a superhydrophobic effect. When the EP on the samples was cured for 8 h and 24 h, the thickness of the rough structure on the coating was increased, as shown in Fig. 6g,g' and h,h'. However, compared with the structure shown in Fig. 6f and f', there was no obvious morphological changes in the surface cluster or granular structure and the quantity of void structures was reduced. It caused the actual CAs of water droplets on the superhydrophobic wood surface to decrease. To conclude, the different curing times led to varied effects in the combination of both EP and SiO<sub>2</sub>-NH<sub>2</sub> particles. As the curing time increased, the EP was further polymerized and the coated SiO<sub>2</sub>-NH<sub>2</sub> particles were gradually accumulated, which promoted the formation of micro-nano structure with cavities or interspace. The number of particles on the surface led to rough structures in various forms, and the contact between water droplets and the wood interface was changed by the type and structures of the pore structures.

In this paper, it was concluded that a model of superhydrophobic surface was prepared by the above method through the analysis of the wood coating configuration in Fig. 6. According to the Cassie-Baxter model theory (Cassie and Baxter 1944; Choi *et al.* 2009), it is believed that there was tension in the solid-liquid-vapor three-phase interface, as depicted in Fig. 7a. When liquid contacted the rough solid surface, macro-roughness occurred and the liquid could not penetrate the harsh surface, resulting in a composite structure being formed by the surface and air. The air was present in pores of the solid-liquid interface and would change the CA of the surface. Based on Young's (Young 1832) equation, it was transformed into the following model equation,

$$\cos \theta' = f_1 \cos \theta_1 + f_2 \cos \theta_2 \quad (1)$$

where  $f_1$  is the surface area fraction occupied by solid-liquid,  $f_2$  is the surface area fraction occupied by solid-vapor, and the  $\theta_1$  and  $\theta_2$  are the CA formed by droplets between the solid and the vapor. The actual CA combined with the micro-rough surface was the  $\theta'$ . Because the CA between the water and air was 180° and  $f_1 + f_2 = 1$  (Cassie 1948), the following condition was also employed,

$$\cos \theta' = f_1 (\cos \theta_1 + 1) - 1 \quad (2)$$

where the smaller  $f_1$  value is, the greater apparent contact angle  $\theta'$ . The wood surface is constructed by a large number of micro-nano structures, which endows the wood surface with a rough morphology and increases the composite contact area of liquid-gas, *i.e.*, the  $f_1$  value of the Wood@EP/SiO<sub>2</sub>-NH<sub>2</sub>&OTS was smaller. Thus, rough surface has a mass of nanoscale pores, which is conducive to obtaining superior superhydrophobic properties (Liu *et al.* 2015a). In this study, the capillary force effect produced on a nano-scale (*i.e.*, the adhesion force) made the water droplets contact with the pores. The SEM images showed that by curing Wood@EP/SiO<sub>2</sub>-NH<sub>2</sub>&OTS for 4 h the surface had nanoscale roughness morphology and tiny air pores. This led to the higher proportion of solid-vapor in the surface area of the wood, and a larger contact angle  $\theta'$  was obtained. Thus, at this

curing time, the hydrophobic property of the wood surface was greater. As shown in Fig. 7(b), this view can be represented by the convex part in the new model with more air pores.

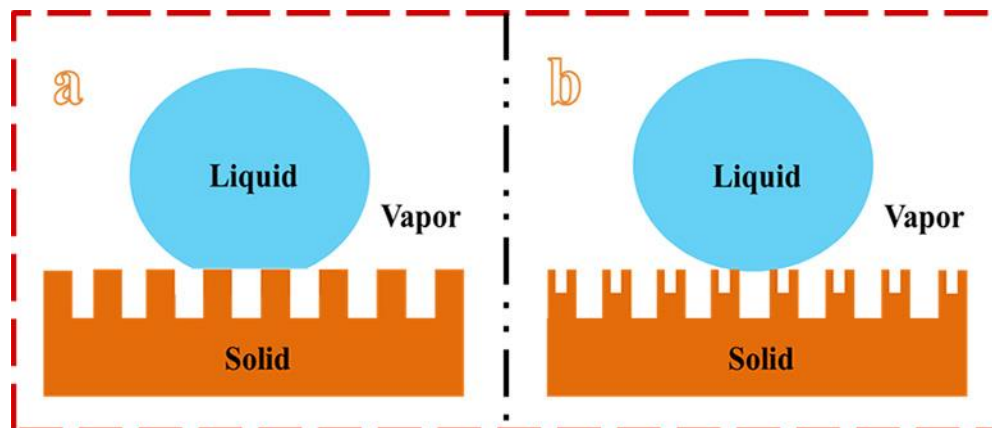


**Fig. 7.** Effect of solid surface structure on wetting performance: (a) Cassie-Baxter's model and (b) Surface structure model prepared by this experimental method

### Simulated Rain Falling Performance Test

To study the stability and durability of superhydrophobic surface, the samples with the best CA and SA in EP curing for 4 h were tested. Simulating naturally mechanical force influenced hydrophobicity and self-cleaning effect of the wood surface have been studied in many years (Liu *et al.* 2013). As depicted in Fig. 8, the CAs of the wood treated with EP still remained in a superhydrophobic state in the initial 9 h, during which the better CA was  $154.3^\circ$  at 3 h.

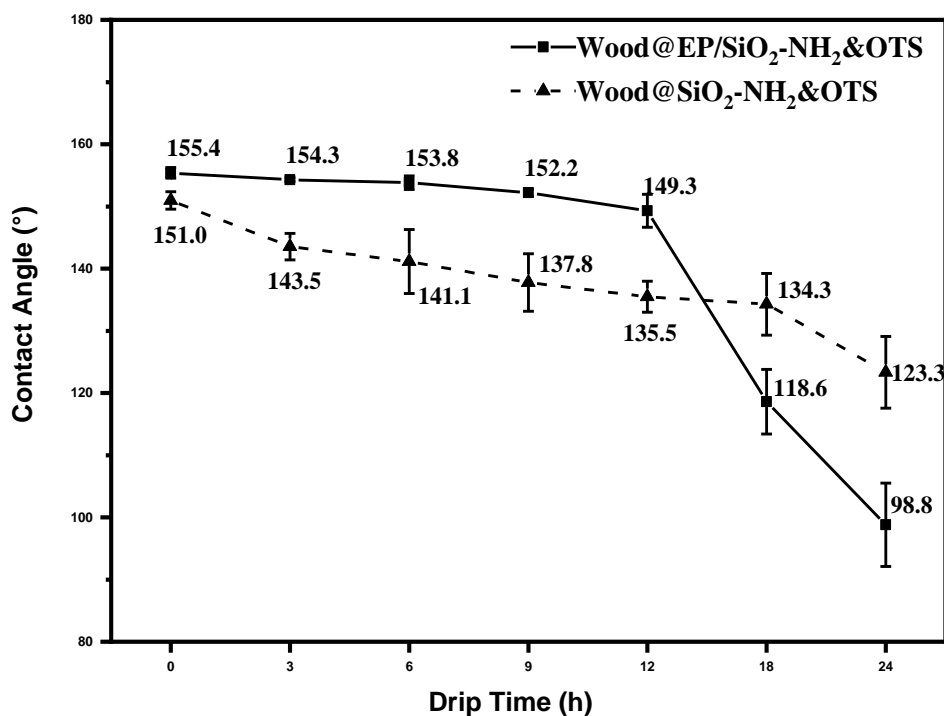


**Fig. 8.** Effect of water drip time on the CAs of the wood surface

With the drip time increasing, regardless of Wood@EP/SiO<sub>2</sub>-NH<sub>2</sub>&OTS or Wood@SiO<sub>2</sub>-NH<sub>2</sub>&OTS, there was a gradual loss of superhydrophobic properties. The reason was that the hydrophobic coating on the wood surface was damaged and the surface wettability was enhanced under the impact of long-term continuous rain. It should be noted that the Wood@SiO<sub>2</sub>-NH<sub>2</sub>&OTS samples lost the superhydrophobic effect after treatment for about 1 h, and the CAs gradually decreased with time. Compared with Wood@SiO<sub>2</sub>-NH<sub>2</sub>&OTS samples, it demonstrated that the stability of the rough coating could be promoted by the EP on the surface.

### Aging Resistance by UV and Heat Test

In the test, the aging resistance of superhydrophobic surface was evaluated by the ultraviolet resistance and heat resistance. Figure 9 shows the surface CAs of droplets on wood samples were irradiated with ultraviolet light (300 W power, 300 nm wavelength) for 3, 6, 9, 12, 18, and 24 h. The CAs of wood decreased sharply after surface testing. The CA of the Wood@EP/SiO<sub>2</sub>-NH<sub>2</sub>&OTS samples after UV irradiation for 24 h dropped to approximately 10°, and the state of the wood surface was changed from hydrophobic to hydrophilic. However, the Wood@SiO<sub>2</sub>-NH<sub>2</sub>&OTS samples changed to a completely wetted state after UV irradiation for 9 h. This indicated that the wood surface was transformed from superhydrophobic to superhydrophilic due to the decomposition of the OTS molecular chain under the action of UV, while the EP in the composite coating could alleviate the transformation process, and the surface roughness also increased.

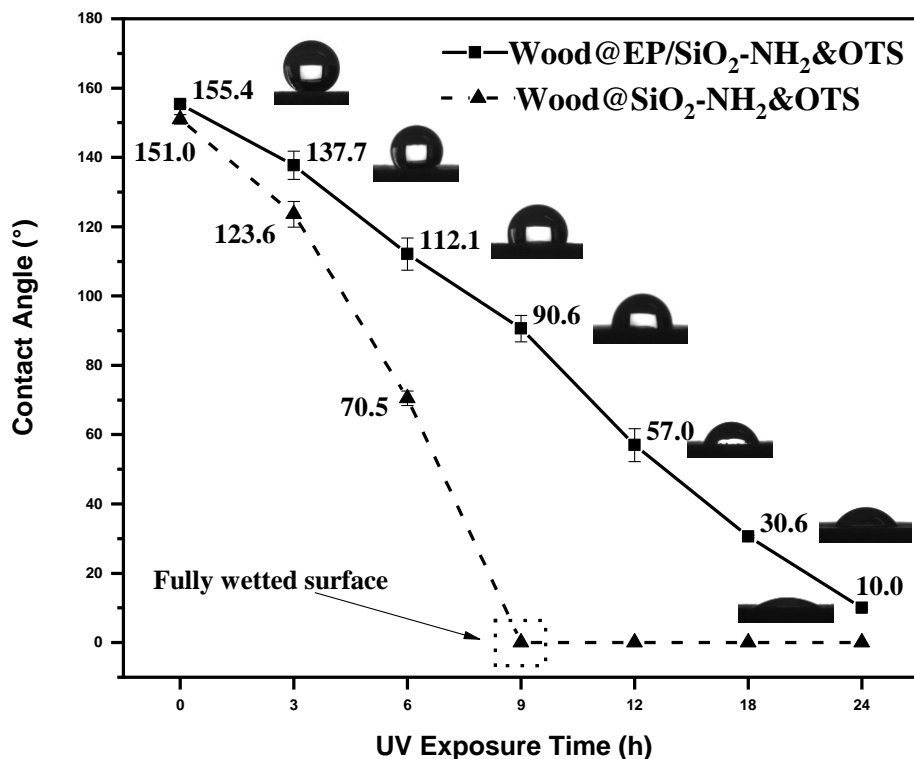
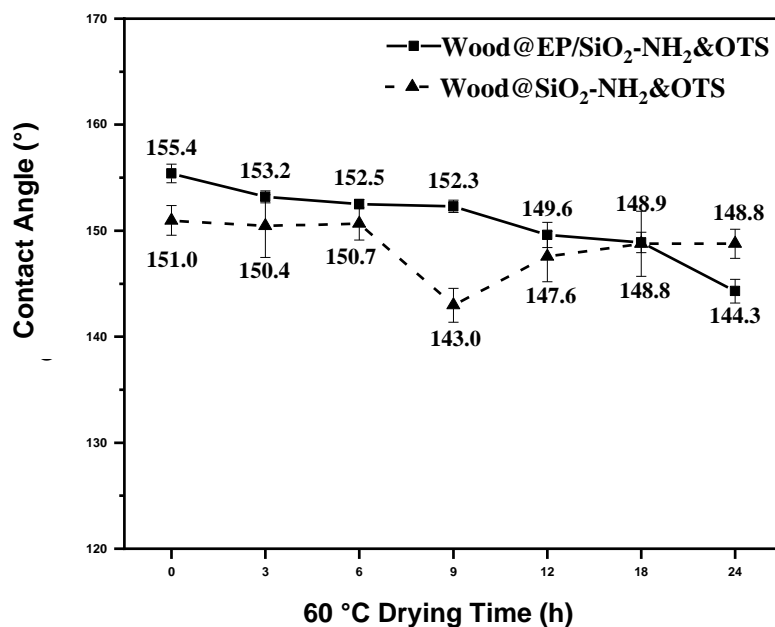


Fig. 9. Effect of UV irradiation time on the CAs of the wood surface

To study the heat resistance of superhydrophobic wood surfaces, the samples were tested at a temperature of 60 °C. According to the data in Fig. 10, the surface CAs of the Wood@EP/SiO<sub>2</sub>-NH<sub>2</sub>&OTS samples were less than 155.4° as the drying time increased. After being dried for 3 h and 6 h, the CAs of the wood surface were 153.2° and 152.5° respectively. This demonstrated that the superhydrophobic state was still achieved. Additionally, in the first three time gradients, the CAs of the Wood@SiO<sub>2</sub>-NH<sub>2</sub>&OTS samples were also greater than 150°. Overall, the surface wettability of the modified wood under high temperature for a long time had little variation. The CAs of the Wood@EP/SiO<sub>2</sub>-NH<sub>2</sub>&OTS decreased slightly, which may be caused by the long-term drying of the EP to further cure the rough surface.



**Fig. 10.** Effect of 60 °C dry time on the CAs of the wood surface

Through comparing the data in Figs. 9 and 10, the influence of heat and UV on the hydrophobic property of the surface coating was analyzed to evaluate the anti-aging property of superhydrophobic wood. Observing the hydrophobic state of the wood surface for 24 h at a temperature of 60 °C, it was found that the wood coating was also affected by temperature. Nevertheless, compared with the surface under ultraviolet irradiation, there was no noticeable change in the CAs of the surface with 60 °C test. Under long-term ultraviolet irradiation, the OTS functional groups on the surface of the wood were decomposed and the rough structure of SiO<sub>2</sub>-NH<sub>2</sub> was destroyed. The hydrophilic group was exposed to the air and increased the adhesion of the droplets to the wood surface, which caused the CA to fall below 150°. In contrast to the Wood@EP/SiO<sub>2</sub>-NH<sub>2</sub>&OTS samples, the surface of the Wood@SiO<sub>2</sub>-NH<sub>2</sub>&OTS samples was completely wetted at 9 h. This indicated that EP could enhance structural aging resistance of the wood surface.

### Determinations of Surface Chemical Stability

The chemical stability of wood surface was determined by superhydrophobic wood samples being soaked in acid-base solutions and different organic solvents. Figure 11

shows the relationship between the effect of acid-base solutions and the CAs of modified wood surface. After immersing the samples in a solution with specific pH values for 24 h, it was found that the CAs of the test wood were lower than the contrast samples. With the increase of the pH value, the CAs of all the samples in the alkaline solution showed a decreasing tendency, but the wood surfaces were still hydrophobic. The results demonstrated that the wood treated with EP had good resistance to acid and alkali degradation. This is due to the fact that the superhydrophobic surface contained chemically stable oxides, such as  $\text{SiO}_2$ , while the EP could stabilize the particles on the wood surface.

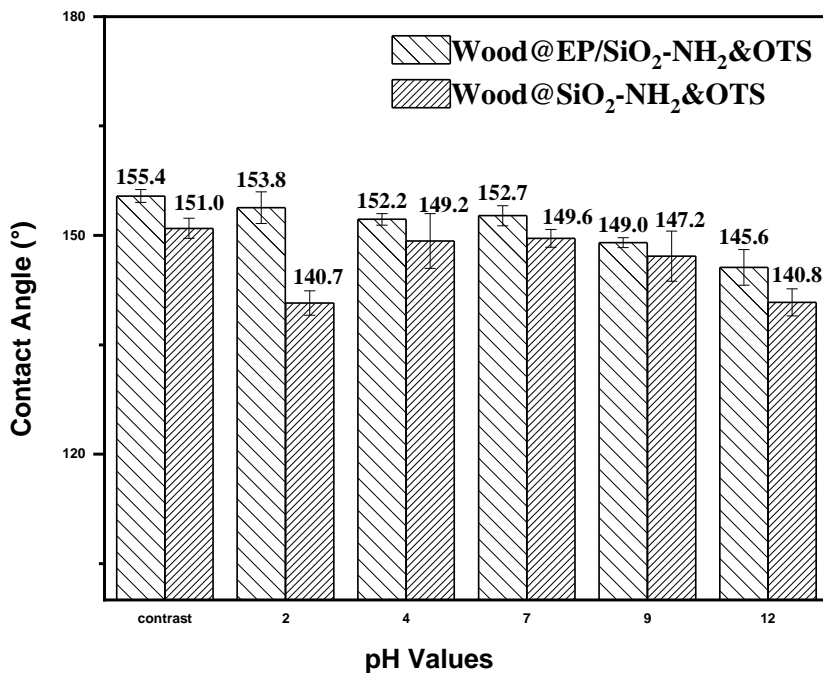


Fig. 11. Effect of acid-based solution on the CAs of the wood surface

As shown in Fig. 12, the Wood@EP/SiO<sub>2</sub>-NH<sub>2</sub>&OTS samples still had good hydrophobic properties after soaking in acetone, alcohol, and n-hexane solution for 24 h. However, the EP and micro-nano structure of the wood surface could hardly bear the dissolving force of N,N-dimethylformamide due to its strong dissolving ability, resulting in the hydrophilic groups on the wood surface being exposed and the surface adhesion to the droplets increased. The CA of the wood surface decreased from 155.4° to 138.0°. Furthermore, after acetone, ethanol, and n-hexane treatment, the surface hydrophobic property of the Wood@SiO<sub>2</sub>-NH<sub>2</sub>&OTS samples were also greatly reduced. However, the CA of the wood surface was improved by immersing in N, N-dimethylformamide solution. This was because some hydroxyl groups on the surface of Wood@ SiO<sub>2</sub>-NH<sub>2</sub>&OTS reacted with N,N-dimethylformamide, resulting in hydrophilic groups decreasing and hydrophobicity increasing.

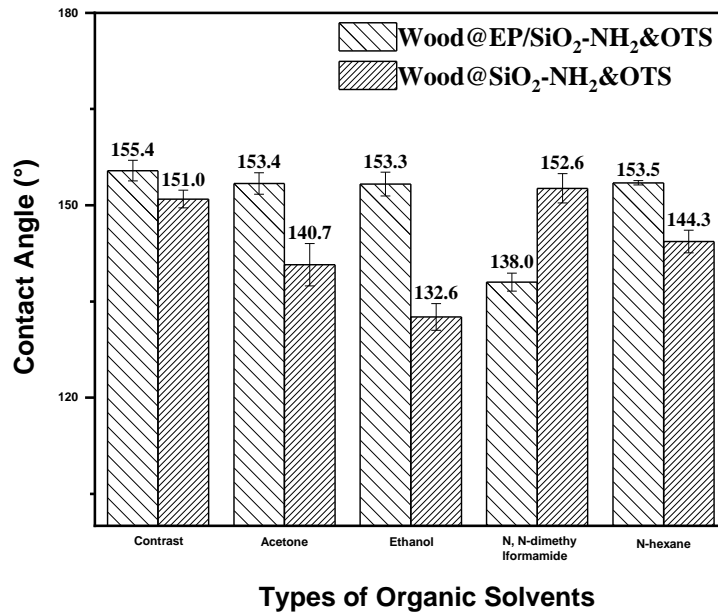


Fig. 12. Effect of organic solvents on the CAs of the wood surface

### Ultrasonic Vibration Test

Figure 13 shows that the CAs of the superhydrophobic wood surface had a declining trend with the increase of ultrasonic vibration time.

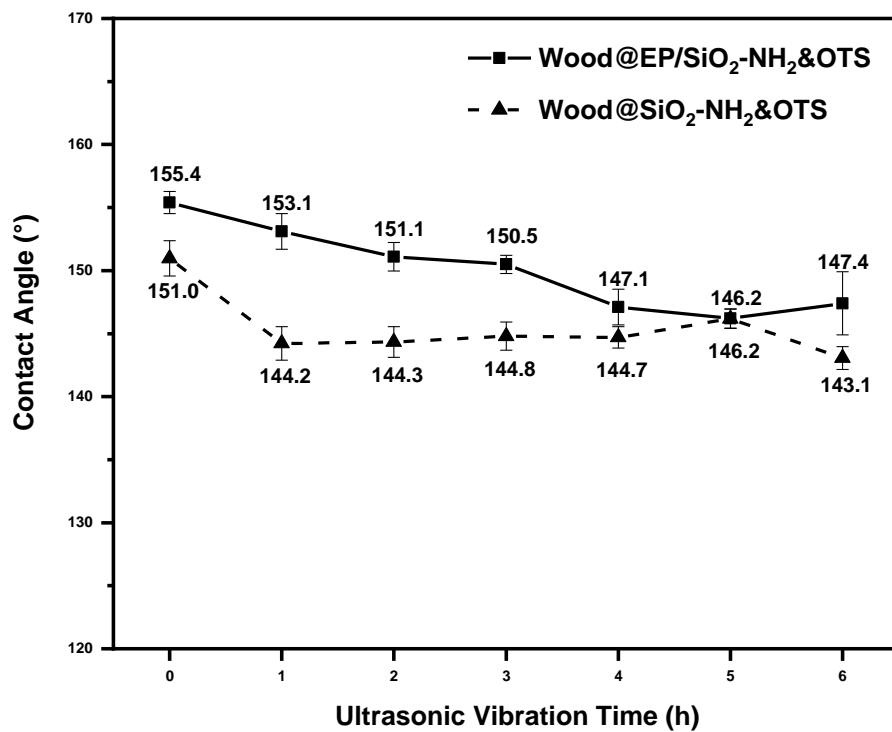


Fig. 13. Effect of ultrasonic oscillation time on the CAs of the wood surface

The CAs of the Wood@SiO<sub>2</sub>-NH<sub>2</sub>&OTS samples were lower than that of the Wood@EP/SiO<sub>2</sub>-NH<sub>2</sub>&OTS samples. This revealed that the nanoparticles of the surface were not tightly bound to the wood and the rough structure was damaged. Through being vibrated with an ultrasonic cleaner, the tight bond between the micro-nano particles and the EP coating was broken down. This exposed the hydrophilic groups of the wood, which resulted in the CAs being decreased, and the wood lost its superhydrophobic properties but retained hydrophobic properties. Clearly, the wood surface can withstand ultrasonic oscillation, which shows that the micro-nanostructures in the superhydrophobic coating are characterized by well stability.

### Abrasion Resistance Test

In the study, the mechanical durability of superhydrophobic wood surface was evaluated by the durability abrasion test. According to the data in Fig. 14, the Wood@EP/SiO<sub>2</sub>-NH<sub>2</sub>&OTS samples were abraded 0 to 5 times, and the wood remained superhydrophobic. The CA of the wood surface was decreased to 140.2° when there was more than 5 times abrasion. While the Wood@SiO<sub>2</sub>-NH<sub>2</sub>&OTS samples only were abraded, and the wood surface lost the superhydrophobic property. The more sawdust left on the sandpaper, the less stable the wood surface coating was. This indicated that the cured epoxy resin has high hardness and strength. The nanoparticles were firmly adhered by chemical bonds to the wood surface and the abrasion resistance was improved.

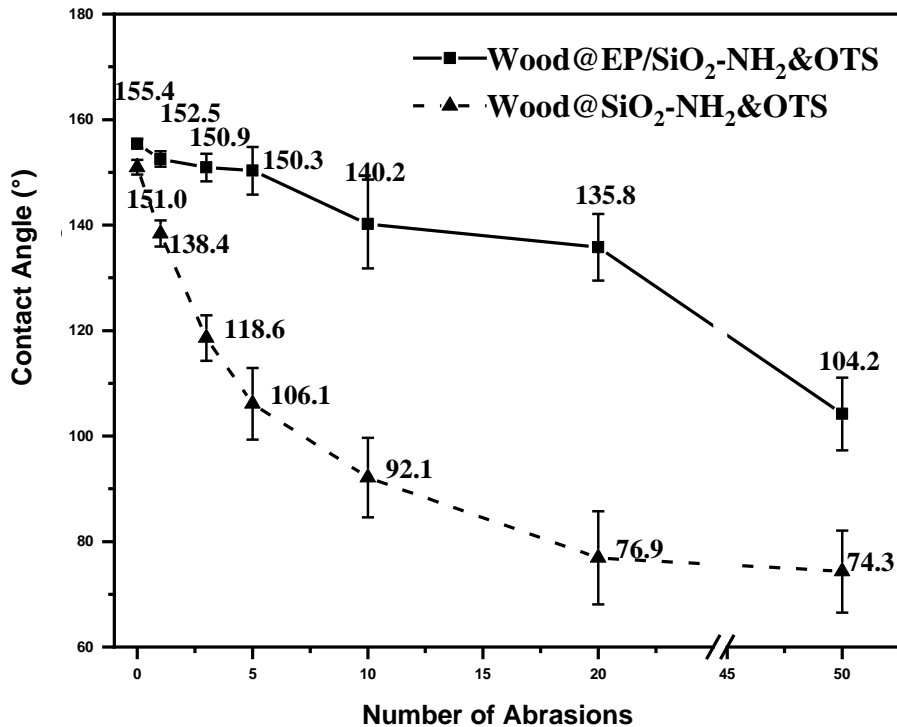


Fig. 14. The effect of sandpaper abrasion on CAs of the wood surface

## CONCLUSIONS

1. A superhydrophobic wood surface was prepared using an epoxy resin with amino-functionalize nano-silica particles (EP/SiO<sub>2</sub>-NH<sub>2</sub>) coating as its substrates, followed by octadecyltrichlorosilane (OTS) reagent modification.
2. Through exploring the effect of EP curing time on the hydrophobic properties of the wood surface, it was found that the surface contact angle of water (CA) reached its highest value of 155.4° with a sliding angle (SA) of 3.9° when the EP cured for 4 h.
3. The scanning electron microscopy (SEM) images showed that the enhancement of the water repellence can be attributed to the abundant pore structures on the Wood@EP/SiO<sub>2</sub>-NH<sub>2</sub>&OTS surface, which increased the proportion of solid-vapor on the surface area of the substrate. For the presence of pores in the solid-liquid interface, a rough structure model with large secondary pores was proposed, which demonstrated that the superhydrophobic property of wood surface was improved.
4. The superhydrophobic wood surface with EP/SiO<sub>2</sub>-NH<sub>2</sub>&OTS coating could tolerate mechanical external forces, such as rain and ultrasonic vibration, and it also had promising resistance to aging and chemical stability.
5. Compared with the Wood@SiO<sub>2</sub>-NH<sub>2</sub>&OTS samples by the rain fall, aging resistance, ultrasonic vibration and abrasion resistance tests of the experiment, it is remarkable that the stability of superhydrophobic surface with EP/SiO<sub>2</sub>-NH<sub>2</sub>&OTS coating was enhanced. This is attributed to the fact that the SiO<sub>2</sub>-NH<sub>2</sub> particles and the wood surface were adhered through the adhesive power of EP, which caused the surface coating to stabilize and the mechanical strength to increased.
6. The aesthetic grain of the wood is not only maintained with the process in this paper, but also the stability and durability of the superhydrophobic surface was improved.

## ACKNOWLEDGMENTS

This research was supported by the Fundamental Research Funds for the National Natural Science Foundation of China (Project No. 31790188).

## REFERENCES CITED

- Aggarwal, P. K., Raghu, N., Kale, A., Vani, C. N., and Chauhan, S. (2015). "Moisture adsorption and absorption behaviour of bio-fiber filled thermoplastic composites," *Journal of the Indian Academy of Wood Science* 12(2), 104-109. DOI: 10.1007/s13196-015-0151-5
- Armingier, B., Gindl-Altmutter, W., Keckes, J., and Hansmann, C. (2019). "Facile preparation of superhydrophobic wood surfaces *via* spraying of aqueous alkyl ketene dimer dispersions," *RSC Adv.* 9(42), 24357-24367. DOI: 10.1039/C9RA03700D
- Barthlott, W., and Neinhuis, C. (1997). "Purity of the sacred lotus, or escape from contamination in biological surfaces," *Planta* 202(1), 1-8. DOI: 10.1007/s004250050096
- Cassie, A. B. D. (1948). "Permeability to water and water vapour of textiles and other



- fibrous materials. Introductory paper,” *Discuss. Faraday Soc.* 3, 239-243. DOI: 10.1039/DF9480300239
- Cassie, A. B. D., and Baxter, S. (1944). “Wettability of porous surfaces,” *T. Faraday Soc.* 40, 546-551. DOI: 10.1039/tf9444000546
- Chen, S., Song, Y. J., and Xu, F. (2018). “Highly transparent and hazy cellulose nanopaper simultaneously with enhanced transparency and a self-cleaning superhydrophobic surface,” *Abstr. Pap. Am. Chem. S.* 6, 5173-5181. DOI: 10.1021/acssuschemeng.7b04814
- Choi, W., Tuteja, A., Mabry, J. M., Cohen, R. E., and McKinley, G. H. (2009). “A modified Cassie–Baxter relationship to explain contact angle hysteresis and anisotropy on non-wetting textured surfaces,” *J. Colloid. Interface Sci.* 339(1), 208-216. DOI: 10.1016/j.jcis.2009.07.027
- Feng, L., Zhang, Y. A., Xi, J. M., Zhu, Y., Wang, N., Xia, F., and Jiang, L. (2008). “Petal effect: A superhydrophobic state with high adhesive force,” *Langmuir* 24(8), 4114-4119. DOI: 10.1021/la703821h
- Han, X., Wang, Z., Zhang, Q., and Pu, J. (2019). “A simple and efficient method to fabricate superhydrophobic wood with enhanced mechanical durability,” *Forests* 10(9), Article number 750. DOI: 10.3390/f10090750
- Jia, S., Liu, M., Wu, Y., Luo, S., Qing, Y., and Chen, H. (2016). “Facile and scalable preparation of highly wear-resistance superhydrophobic surface on wood substrates using silica nanoparticles modified by VTES,” *Appl. Surf. Sci.* 386, 115-124. DOI: 10.1016/j.apsusc.2016.06.004
- Kumar, A., Richter, J., Tywoniak, J., Hajek, P., Adamopoulos, S., Šegedin, U., and Petrič, M. (2018). “Surface modification of Norway spruce wood by octadecyltrichlorosilane (OTS) nanosol by dipping and water vapour diffusion properties of the OTS-modified wood,” *Holzforschung* 72(1), 45-56. DOI: 10.1515/hf-2017-0087
- Liu, C., Wang, S., Shi, J., and Wang, C. (2011). “Fabrication of superhydrophobic wood surfaces via a solution-immersion process,” *Appl. Surf. Sci.* 258(2), 761-765. DOI: 10.1016/j.apsusc.2011.08.077
- Liu, F., Wang, S., Zhang, M., Ma, M., Wang, C., and Li, J. (2013). “Improvement of mechanical robustness of the superhydrophobic wood surface by coating PVA/SiO<sub>2</sub> composite polymer,” *Appl. Surf. Sci.* 280, 686-692. DOI: 10.1016/j.apsusc.2013.05.043
- Liu, F., Gao, Z., Zang, D., Wang, C., and Li, J. (2015a). “Mechanical stability of superhydrophobic epoxy/silica coating for better water resistance of wood,” *Holzforschung* 69(3), 367-374. DOI: 10.1515/hf-2014-0077
- Liu, Y., Liu, J., Li, S., Wang, Y., Han, Z., and Ren, L. (2015b). “One-step method for fabrication of biomimetic superhydrophobic surface on aluminum alloy,” *Colloids Surf. A- Physicochem. Eng. Asp.* 466, 125-131. DOI: 10.1016/j.colsurfa.2014.11.017
- Liu, H. D., Zhang, H., Pang, J., Ning, Y. J., Jia, F., Yuan, W. F., Gu, B., and Zhang, Q. P. (2019). “Superhydrophobic property of epoxy resin coating modified with octadecylamine and SiO<sub>2</sub> nanoparticles,” *Mater. Lett.* 247, 204-207. DOI: 10.1016/j.matlet.2019.03.128
- Lu, Z., Xu, L., He, Y., and Zhou, J. (2019). “One-step facile route to fabricate functionalized nano-silica and silicone sealant based transparent superhydrophobic coating,” *Thin Solid Films* 692, Article number 137560. DOI: 10.1016/j.tsf.2019.137560

- Lukawski, D., Lekawa-Raus, A., Lisiecki, F., Koziol, K., and Dudkowiak, A. (2018). "Towards the development of superhydrophobic carbon nanomaterial coatings on wood," *Prog. Org. Coat.* 125, 23-31. DOI: 10.1016/j.porgcoat.2018.08.025
- Neinhuis, C., and Barthlott, W. (1997). "Characterization and distribution of water-repellent, self-cleaning plant surfaces," *Ann. Bot.-London* 79(6), 667-677.
- Parvate, S., Dixit, P., and Chattopadhyay, S. (2020). "Superhydrophobic surfaces: Insights from theory and experiment," *J. Phys. Chem. B* 124(8), 1323-1360. DOI: 10.1021/acs.jpcc.9b08567
- Psarski, M., Pawlak, D., Grobelny, J., and Celichowski, G. (2019). "Relationships between surface chemistry, nanotopography, wettability and ice adhesion in epoxy and SU-8 modified with fluoroalkylsilanes from the vapor phase," *Appl. Surf. Sci.* 479, 489-498. DOI: 10.1016/j.apsusc.2019.02.082
- Sahoo, B. N., and Kandasubramanian, B. (2014). "Recent progress in fabrication and characterisation of hierarchical biomimetic superhydrophobic structures," *RSC Adv.* 4(42), Article number 22053. DOI: 10.1039/c4ra00506f
- Shah, S. M., Zulfiqar, U., Hussain, S. Z., Ahmad, I., Habib-ur-Rehman, Hussain, I., and Subhani, T. (2017). "A durable superhydrophobic coating for the protection of wood materials," *Mater. Lett.* 203, 17-20. DOI: 10.1016/j.matlet.2017.05.126
- Su, X., Li, H., Lai, X., Zhang, L., Liang, T., Feng, Y., and Zeng, X. (2017). "Polydimethylsiloxane-based superhydrophobic surfaces on steel substrate: Fabrication, reversibly extreme wettability and oil-water separation," *ACS Appl. Mater. Inter.* 9(3), 3131-3141. DOI: 10.1021/acsami.6b13901
- Tenjimbayashi, M., and Shiratori, S. (2014). "Highly durable superhydrophobic coatings with gradient density by movable spray method," *J. Appl. Phys.* 116(11), Article number 114310. DOI: 10.1063/1.4895777
- Tu, K., Wang, X., Kong, L., and Guan, H. (2018). "Facile preparation of mechanically durable, self-healing and multifunctional superhydrophobic surfaces on solid wood," *Mater. Design* 140, 30-36. DOI: 10.1016/j.matdes.2017.11.029
- Tuong, V. M., Huyen, N. V., Kien, N. T., and Dien, N. V. (2019). "Durable epoxy@ZnO coating for improvement of hydrophobicity and color stability of wood," *Polymers* 11(9), Article number 1388. DOI: 10.3390/polym11091388
- Wagner, T., Neinhuis, C., and Barthlott, W. (2010). "Wettability and contaminability of insect wings as a function of their surface sculptures," *Acta Zool.-Stockholm* 77(3), 213-225. DOI: 10.1111/j.1463-6395.1996.tb01265.x
- Wang, F., Pi, J., Song, F., Feng, R., Xu, C., Wang, X.-L., and Wang, Y.-Z. (2020a). "A superhydrophobic coating to create multi-functional materials with mechanical/chemical/physical robustness," *Chem. Eng. J.* 381, Article ID 122539. DOI: 10.1016/j.cej.2019.122539
- Wang, J., Lu, Y., Chu, Q., Ma, C., Cai, L., Shen, Z., and Chen, H. (2020b). "Facile construction of superhydrophobic surfaces by coating -0/silica composite on a modified hierarchical structure of wood," *Polymers-Basel* 12(4), Article number 813. DOI: 10.3390/polym12040813
- Wang, K., Dong, Y., Zhang, W., Zhang, S., and Li, J. (2017). "Preparation of stable superhydrophobic coatings on wood substrate surfaces via mussel-inspired polydopamine and electroless deposition methods," *Polymers-Basel* 9(6), Article number 218. DOI: 10.3390/polym9060218
- Wang, S., Wang, C., Liu, C., Zhang, M., Ma, H., and Li, J. (2012). "Fabrication of superhydrophobic spherical-like  $\alpha$ -FeOOH films on the wood surface by a

- hydrothermal method,” *Colloids Surf. A- Physicochem. Eng. Asp.* 403, 29-34. DOI: 10.1016/j.colsurfa.2012.03.051
- Wang, S., Liu, C., Liu, G., Zhang, M., Li, J., and Wang, C.. (2011). “Fabrication of superhydrophobic wood surface by a sol-gel process,” *Appl. Surf. Sci.* 258(2), 806-810. DOI: 10.1016/j.apsusc.2011.08.100
- Wang, Y., Tang, Z., Lu, S., Zhang, M., Liu, K., Xiao, H., Huang, L., Chen, L., Wu, H., and Ni, Y. (2020c). “Superhydrophobic wood grafted by poly(2-(perfluorooctyl)ethyl methacrylate) via ATRP with self-cleaning, abrasion resistance and anti-mold properties,” *Holzforschung* 74(8), 799-809. DOI: 10.1515/hf-2019-0184
- Wang, Y., Yan, W., Frey, M., Vidiella del Blanco, M., Schubert, M., Adobes-Vidal, M., and Cabana, E. (2019). “Liquid-like SiO<sub>2</sub>-g-PDMS coatings on wood surfaces with underwater durability, antifouling, antimudge, and self-healing properties,” *Advanced Sustainable Systems* 3(1), Article ID 1800070. DOI: 10.1002/adsu.201800070
- Wu, Y., Jia, S., Qing, Y., Luo, S., and Liu, M. (2016). “A versatile and efficient method to fabricate durable superhydrophobic surfaces on wood, lignocellulosic fiber, glass, and metal substrates,” *J. Mater. Chem. A* 4(37), 14111-14121. DOI: 10.1039/C6TA05259B
- Xing, Y., Xue, Y., Song, J., Sun, Y., Huang, L., Liu, X., and Sun, J. (2018). “Superhydrophobic coatings on wood substrate for self-cleaning and EMI shielding,” *Appl. Surf. Sci.* 436, 865-872. DOI: 10.1016/j.apsusc.2017.12.083
- Xu, H. Y., Li, B., Han, X., Wang, Y., Zhang, X. R., and Komarneni, S. (2019). “Synergic enhancement of the anticorrosion properties of an epoxy coating by compositing with both graphene and halloysite nanotubes,” *J. Appl. Polym. Sci.* 136(21), Article ID 47562. DOI: 10.1002/app.47562
- Xue, C.-H., Jia, S.-T., Zhang, J., and Tian, L.-Q. (2009). “Superhydrophobic surfaces on cotton textiles by complex coating of silica nanoparticles and hydrophobization,” *Thin Solid Films* 517(16), 4593-4598. DOI: 10.1016/j.tsf.2009.03.185
- Yang, R., Wang, S., Zhou, D., Zhang, J., Lan, P., and Jia, C. (2018). “Construction of hydrophobic wood surface and mechanical property of wood cell wall on nanoscale modified by dimethyldichlorosilane,” *IOP Conf. Ser.-Mat. Sci.* 301(1), Article ID 012051. DOI: 10.1088/1757-899X/301/1/012051
- Yang, Y., He, H., Li, Y., and Qiu, J. (2019). “Using nanoimprint lithography to create robust, buoyant, superhydrophobic PVB/SiO<sub>2</sub> coatings on wood surfaces inspired by red roses petal,” *Entific Reports* 9(1), Article number 9961. DOI: 10.1038/s41598-019-46337-y
- Yang, Y., Shen, H., and Qiu, J. (2020). “Fabrication of biomimetic robust self-cleaning superhydrophobic wood with canna-leaf-like micro/nanostructure through morphogenetic method improved water-, UV-, and corrosion resistance properties,” *J. Mol. Struct.* 1219, Article number 128616. DOI: 10.1016/j.molstruc.2020.128616
- Yi, Z., Zhao, B., Liao, M., and Qin, Z. (2020). “Fabrication of superhydrophobic wood surface by etching polydopamine coating with sodium hydroxide,” *Coatings* 10(9), Article number 847. DOI: 10.3390/coatings10090847
- Young, T. (1832). “An essay on the cohesion of fluids,” *Proc. R. Soc. Lond.* 1, 171-172. DOI: 10.1098/rspl.1800.0095
- Zhan, Z. B., Garcell, E. M., and Guo, C. L. (2019). “Robust mold fabricated by femtosecond laser pulses for continuous thermal imprinting of superhydrophobic surfaces,” *Mater. Res. Express* 6(7), Article ID 075011. DOI: 10.1088/2053-

1591/ab10c6

Zhao, M., Tao, Y., Wang, J., and He, Y. (2020). "Facile preparation of superhydrophobic porous wood for continuous oil-water separation," *Journal of Water Process Engineering* 36, Article number 101279. DOI: 10.1016/j.jwpe.2020.101279

Zhou, H., Chen, R., Liu, Q., Liu, J., Yu, J., Wang, C., Zhang, M., Liu, P., and Wang, J. (2019). "Fabrication of ZnO/epoxy resin superhydrophobic coating on AZ31 magnesium alloy," *Chem. Eng. J.* 368, 261-272. DOI: 10.1016/j.cej.2019.02.032

Article submitted: November 4, 2020; Peer review completed: January 24, 2021; Revised version received and accepted: March 1, 2021; Published: March 15, 2021.

DOI: 10.15376/biores.16.2.3235-3254